Dual-detection approach for charge variant analysis of monoclonal antibody combination products using imaged capillary isoelectric focusing

Jason Candreva[1,*], Abbie L. Esterman[1,*], Derek Ge[2], Pritesh Patel[1], Shannon C. Flagg[1], Tapan K. Das[1], Xue Li[1]

[1]Biologics Development , Bristol Myers Squibb, New Brunswick, NJ.

[2] University of Michigan, Ann Arbor, MI.

* The first two authors contributed equally to this publication.

Correspondence should be addressed to the following author(s):

Xue Li, Biologics Development, Bristol Myers Squibb , 1 Squibb Drive, New Brunswick, NJ 08901 USA.
Email: xue.li1@bms.com

Received: 02/06/2022; Revised: 05/16/2022; Accepted: 05/21/2022

This article has been accepted for publication and undergone full peer review but has not been through the copyediting, typesetting, pagination and proofreading process, which may lead to differences between this version and the Version of Record. Please cite this article as doi: 10.1002/elps.202200026.

This article is protected by copyright. All rights reserved.

ORCID (Xue Li): https://orcid.org/0000-0002-9850-5132

Keywords: capillary electrophoresis, charge variants, combination therapy, iCIEF, monoclonal antibody

Abbreviations: ABS, absorbance; FDC, fixed-dose combination; FL, fluorescence; ICH, International Conference on Harmonization; iCIEF, imaged capillary isoelectric focusing; QC, quality control; UV, ultraviolet

Abstract

The clinical benefits of treatments with combination of two or more therapeutic mAbs have emerged in recent years. Imaged capillary isoelectric focusing (iCIEF) is a frequently-used technology in the biopharmaceutical industry for charge variant analysis of protein therapeutics. However, with the wide concentration ranges of combination products, one component may fall within the linear detection range while the other does not. Here, we report a novel methodology to explore charge variants of mAb mixtures using multiple detection techniques simultaneously. We use UV (ultraviolet) to monitor the charge variants of the high-concentration component, and native fluorescence to monitor the variants of the low-concentration one. Charge variants of mixtures that span 40-fold in ratio differences can be accurately quantified with this approach. In contrast to the conventional methods, it is not necessary to prepare and analyze two samples at different concentrations and combine the results for combination product testing. Additionally, the use of fluorescence detection enables charge variant analysis of highly potent/low abundant mAbs in a mixture. This methodology is more QC friendly and efficient for charge variant analysis of combination products with wide ratios.

This article is protected by copyright. All rights reserved.

Introduction

Therapeutic proteins manufactured in mammalian cell culture are a heterogeneous population, containing fragments, aggregates, and variants with PTMs, such as glycosylation, sialylation, deamidation, glycation, and oxidation [1–6]. These PTMs impact the charge of amino acid residues, resulting in changes of acid dissociation constant (pKa) and surface charge [6]. Control of charge variants has been an expectation from health authorities. Robust methods with high resolution are required to monitor the charge profile to support product and process development [2,7,8].

Compared to other technologies used to monitor charge variants, such as ion-exchange chromatography (IEX) [9–12], CZE [12,13], and traditional slab-gel IEF [14,15], Imaged capillary isoelectric focusing (iCIEF) offers a number of advantages for monitoring charge variants of biomolecules [7,8,12,16–21]. The iCIEF technology is amenable to platform conditions for molecules with a wide range of pI values, as only minimal method development is needed for the transition amongst typical mAb molecules. Additionally, the introduction of dual detection of native fluorescence and ultraviolet (UV) provides greater sensitivity of low abundant species with an increased dynamic linear range [12,22,23].

During iCIEF analysis, the separation occurs in a capillary, and is monitored in real time using a charge-coupled device (CCD) camera [8,22]. To mitigate protein aggregation and precipitation of biomolecules at their pI's, additives such as urea are added to increase solubility [19,21]. Since a mobilization step is not required, the separation can be monitored in real-time, decreasing the time for method development [17]. The data obtained from iCIEF analysis includes the apparent experimental pI of each isoform, as well as ratiometric quantification of each species. Typically, the percentages of acidic (lower pI) and basic (higher pI) variants as compared to the main isoform species are reported [6,16,18,24,25].

Recently, combination therapies have garnered increased efforts from the pharmaceutical industry enabling development of patient-centric dosage forms, especially in the treatment of cancer. More than 1100 clinical trials of combination therapies have been documented for immuno-oncology treatments [26]. The treatment regimens include sequential [27–31], co-administration, or fixed dose combination products (FDC) [32,33]. For instance, immune checkpoint blockade of tumors is a novel strategy in clinical oncology using FDC products. In patients with advanced melanoma, treatment with relatlimab plus nivolumab FDC achieved a significant benefit compared to treatment with nivolumab monotherapy [32]. Additionally, the combination of pertuzumab and trastuzumab FDC to block HER2 gene overexpression in breast cancer has proven beneficial [33].

Aimed at both co-administration and FDC products, enhanced analytical methods are needed to monitor product quality attributes for use-time studies and program life-cycles [34,35]. The

This article is protected by copyright. All rights reserved.

conventional iCIEF and IEX assays using UV detection lack the needed sensitivity [36] and dynamic range to simultaneously quantify charge variants of multiple components in wide ratios, such as FDC products with ratios ranging from 1:6 to 1:40. In a recent publication, Li et al. report the use of fluorescence detection to monitor charge variants of low levels of erythropoietin in simulated drug product formulations [37]. Another drawback of CIEF technology is lack of resolution among co-formulated molecules with similar pI values. Cao et al. report a CIEF method for monitoring charge variants in co-formulated mAb products. However, peptide mapping was needed to quantify the acidic species of the higher pI mAb when the ratios were wider than 1:1 due to the closely related pI of the two mAbs which could not be adequately resolved by CIEF [38]. Many of the challenges associated with traditional CIEF are also true of CZE, which makes the technology less than ideal in developing a method for robust analytical control. Goyon et al. report a CZE method to quantify the charge variants in mAb mixtures, including a mixture of ipilimumab and nivolumab, but only at 1:1 ratio [13].

In this paper, we discuss the development, qualification, and application of a novel iCIEF methodology to simultaneously and accurately quantify the acidic and basic charge variants of FDC products consisting of two mAbs with differing pI's, with wide ratios up to 1:40. The limited dynamic range of sensitivity of conventional iCIEF methods is overcome by taking advantage of the dual detection systems and the ability to simultaneously monitor native fluorescence and UV absorbance. Due to the many inherent advantages of iCIEF technology and the dual detection systems, the resulting method is QC (quality control) friendly with suitable acceptance criteria for sensitivity, specificity, linearity, and repeatability, in accordance with the International Conference on Harmonization (ICH) guidelines [39].

Materials and methods

Materials

Maurice iCE system with Compass software, methyl cellulose, pI markers, Maurice electrolyte solution and Fc cartridges were purchased from ProteinSimple (Santa Clara, CA). Urea was sourced from Millipore Sigma (St. Louis, MO) and Pharmalytes from GE Healthcare/Millipore Sigma (St. Louis, MO). Antibodies of IgG1 and IgG4 isotypes were provided by Bristol Myers Squibb. Empower v3 software was supplied by Waters (Milford, MA) and JMP software version 13.1.0. by SAS (Cary, North Carolina). Corresponding monotherapy antibodies were used as reference materials in this study for FDC mixtures.

This article is protected by copyright. All rights reserved.

Methods

iCIEF sample preparation

Individual mAb samples were diluted using ultrapure water (Milli-Q) to varying working concentrations (up to 10.0 mg/mL) for linearity experiments. For analysis of FDC products, the individual mAbs were mixed at differing mass ratios (from 40:1 to 1:40) and samples were prepared at a working concentration of up to 10.0 mg/mL. The samples were then diluted 1:10 (final concentration up to 1.0 mg/mL) in molecule specific master mixes consisting of 2–4 M urea, 0.35% methyl cellulose, 4% Pharmalytes (mixtures of 3–10, 5–8, and 8–10.5), 5 mM Arginine (only for mAb1:mAb3), and pI markers. The master mix component compositions were optimized using different ratios of Pharmalytes and additives for each pair of molecules to maximize resolution and ensure no overlap of the charge variants from the two molecules. Each new condition was further tested to verify no changes in the relative abundance of the acidic, main, and basic regions were observed as compared to the values obtained using qualified methods for each molecule. For linearity studies, three independent preparations at each level were injected.

Maurice instrument parameters

The separation occurs in a fluorocarbon-coated silica capillary (5 cm long with 100 µm inner diameter), and the entire capillary is monitored in real time using a CCD camera imaging with both native fluorescence and/or absorbance at 280 nm. The Maurice instrument with Compass software were initialized as per vendor instructions. Samples were placed on the autosampler and maintained at 10°C during the run. The injections were pre-focused at 1500 V for 1 min and focused at 3000 V for 10 min. Raw data was collected using dual-detection imaging of the whole capillary, simultaneously monitoring UV absorbance at 280 nm and native fluorescence emission collected from 320 nm to 450 nm with 20 seconds exposure. Maurice separation and detection parameters were optimized during method development. Various exposure times were evaluated (5–20 seconds), with 20 seconds being optimal.

Data Analysis

Calibrated data from Compass software was exported to EMPOWER v3. Electropherograms, peak Integration and peak area quantification of acidic variants, basic variants, and main peak area percentages were performed using EMPOWER v3. Linear regressions and fit analysis were performed using JMP.

Results and discussion

With the emergence of co-administration and FDC biologic products, especially in the field of oncology, the need is critical for advanced analytical methods to monitor charge attributes in

This article is protected by copyright. All rights reserved.

mixtures of multiple molecules. To our knowledge, this is the first report on a method to directly measure charge variants of combination products with ratios ranging from 1:1 to 1:40 using only iCIEF. The success of our methodology is demonstrated with proof-of-concept experiments using two model mixtures with different mAb combinations of IgG1 and IgG4 isotypes (Model 1: mAb1 & mAb2; Model 2: mAb1 & mAb3) mixed in ratios ranging from 1:40 to 40:1 (final concentrations range from ~ 0.02 mg/mL to ~ 0.98 mg/mL). These model molecules represent mAbs with pI values ranging from 6 to 9.

Limits of Detection by UV Absorbance

As shown in the electropherogram of the 1:1 mixture of mAb1:mAb2 (**Figure 1)**, there is no overlap between the last basic peak of mAb2 and the first acidic peak of mAb1. It is important to ensure that no overlap of the variant peaks of mAb1 and mAb2 ensues, even in the case of peak drift or new peak formation due to a degradation event. Traditional UV detection is not sensitive enough for the lower-concentration species in the FDC product with ratios wider than 1:6 to 6:1, while signal of the more abundant species may have saturated the detector. However, as shown in **Figure 1**, the less-abundant mAb can be reliably quantified using fluorescence detection. By taking advantage of the dual detection, the charge variants of each mAb in the wide ratio FDC product can be quantified in a single injection. Additionally, the use of fluorescence detection eliminated the known interference of histidine in formulation buffer using UV detection, as histidine has negligible signal at the 320–450 nm wavelength range used in native fluorescent mode [40,41].

Dynamic linear range of absorbance and native fluorescence

Using the traditional iCIEF approach, in order to analyze ratios wider than 1:6 and 6:1, two sample preparations are required — one to quantify the more-abundant species at the nominal sample concentration; and a second at a higher sample concentration in order to have enough signal for the less-abundant species, meanwhile saturating the detector of the more-abundant species. This traditional protocol has two disadvantages: 1) significantly overloading the capillary with high-concentration sample often results in sample precipitation and capillary clogging, and 2) it is not QC-friendly as the analyst has to prepare and analyze two samples and combine the data for meaningful results. Both concerns can be alleviated by employing our proposed dual detector approach.

The advantage of monitoring the capillary with absorbance and fluorescence simultaneously is portrayed in **Figure 1**. However, preliminary evaluation is needed to determine which detection mode to use for the quantification of each component in the mixture. In some cases, where the ratio is closer to 1:1, absorbance will be sufficient to quantify both components. With wider ratio products, between 1:6 and 1:40, fluorescence detection may be required to accurately quantify the lower abundant species. In order to determine which detection mode is appropriate, linearity is performed with both absorbance and fluorescence. The concentration of the component to be measured should be within the acceptable linear range of the detection mode, taking into

This article is protected by copyright. All rights reserved.

consideration the lower abundance of acidic and basic variants, to ensure method robustness within the expected performance variance. In this study, the upper limit for absorbance linearity of mAb1 and mAb2 is ~1.0 mg/mL, and 0.667 mg/mL for mAb3 due to its higher extinction coefficient.

As an example, **Figure 2** shows the representative electropherograms of mAb3 across the entire linear range, which ranges from 0.088 to 0.667 mg/mL for UV, and 0.017 to 0.088 mg/mL for fluorescence. The end points of the range (0.017 mg/mL to 0.667 mg/mL) represent a 1:40 dilution. The electropherograms show that the profiles and relative percent peak areas are consistent across the mass range using both detection modes. Data qualifying the method following ICH guidelines for repeatability, accuracy, and precision are presented below.

Experiments were performed to determine the linear range of each component of the mAb mixtures. The criteria assessed include visually comparable profiles, accuracy of 80–120% recovery (the recovery is calculated by comparing experimental values to theoretical values determined by the regression line), precision (%RSD ≤ 5.0% for % main peak area; %RSD ≤ 15% for %peak area of variant species), and linearity ($R^2 \geq 0.98$). The absorbance linearity of the main peak area of mAb1 and mAb2 is shown in **Figure 3A** and **Figure 3B**. Although the data appears to be linear across wide concentration ranges ($R^2 \geq 0.99$), there is a loss of accuracy at lower and upper concentrations of the ranges. By narrowing the ranges at the lower concentrations (e.g., 0.13 mg/mL instead of 0.03 mg/mL for mAb1; 0.11 mg/mL instead of 0.02 mg/mL for mAb2), recovery is improved. Furthermore, by narrowing the concentration range of mAb1 from 0.03–0.98 to 0.06–0.65 mg/mL, the recovery of the main peak improved from 70–107% to 98–103%. This is because the signal is now within the linear range of the UV detector and is an example of how R^2 is not the only indicator of linearity across large mass ranges. Similarly, for mAb2, the percent recovery was improved by narrowing the concentration range.

Table 1. Linear concentration ranges for mAb1, mAb2, and mAb3 with absorbance (ABS) and fluorescence with 20 seconds exposure (FL). Ranges of relative percent peak area for acidic, main, and basic are given for data obtained across the final sample concentration range (after master mix addition). Ref values reported from the Certificate of Analysis.

	Range (mg/mL)	Main Peak R^2	%Recovery	% Acidic	% Main	% Basic
mAb1 ABS	0.13–0.98	0.9937	94–111	27.4–33.9	59.1–66.8	7.1–8.2
mAb1 FL	0.03–0.13	0.9999	98–102	28.7–31.1	61.1–63.8	7.4–7.8
mAb1 Ref	–	–	–	31.0	61.0	7.0
mAb2 ABS	0.11–0.99	0.9989	96–103	10.6–11.4	50.3–50.8	38.3–38.8

This article is protected by copyright. All rights reserved.

mAb2 FL	0.02–0.11	0.9991	97–102	10.3–11.0	49.2–50.6	39.1–39.8
mAb2 Ref	–	–	–	10.6	50.5	38.9
mAb3 ABS	0.06–0.67	0.9983	91–105	16.9–18.5	41.5–42.6	39.2–41.2
mAb3 FL	0.02–0.06	0.9978	99–102	15.4–16.7	41.8–42.7	41.4–42.6
mAb3 Ref	–	–	–	16.9	41.9	41.2

The fluorescence linearity was evaluated using 20 seconds of exposure across 0.02–0.99 mg/mL concentration range. Fluorescence linearity of the mAb2 main peak is shown in **Figure 3C**. Across the entire range, the signal begins to get saturated at high concentrations. However, the signal is linear at the low concentrations of the range 0.02–0.11 mg/mL, as shown by the zoomed-in view, and the lower concentration range was determined to be linear as shown in **Table 1**. The linear range for each detection mode, determined from both the absorbance and fluorescence data, is also shown in **Table 1**. These results demonstrate the feasibility of using absorbance for charge variant analysis at relatively higher concentration ranges and fluorescence at relatively lower concentration levels.

Proof-of-concept 1:40 to 40:1 FDC

Once the linearity ranges with both detection modes have been determined, evaluation of the method performance parameters is the next key step. To demonstrate the applicability of this method to accurately quantitate wide ranges of mAb mixtures, two mAb combinations ranging from 1:40 to 40:1 were tested. The results of the mixtures of mAb1 and mAb2 are shown in **Figure 4A**. Fluorescence detection was used in cases where one species was significantly less abundant than the other, as denoted by the asterisk in **Figure 4A**. The fluorescence values fall within the linear range, which was determined for each molecule during the method development phase. For mAb1 and mAb2, the ranges were selected based on the above studies on the linearity of each detection mode. Across the entire range, the quantification of the acidic, main, and basic peaks of each component was accurate and repeatable. Three independent preparations at each level resulted in RSD% values ≤ 4.9% for all variant species measured, and ≤ 0.7% for the main peak. The RSD% values are well within the typical repeatability acceptance criteria of 15.0% and 5.0%, respectively. Accuracy also passed typical acceptance criteria (%Recovery of 80–120% for main peak and 70–130% for variant species). The acceptance criteria are based on internal guideline for method qualification.

The results for FDC products of mAb1 and mAb3 are shown in **Figure 4B**. The RSD% values were ≤ 4.4% for all variant species measured, and ≤ 1.6% for the main peaks (see the above paragraph for the acceptance criteria). For this pair of mAbs, the acceptable range is limited to FDC ratios of 1:25 to 40:1. The absorbance linearity range of mAb3 did not support concentrations of mAb3 in FDC products wider than 1:25 (i.e., 1:40), as mAb3 saturates the UV detector at concentrations above

This article is protected by copyright. All rights reserved.

0.667 mg/mL. To accurately measure ratios below 1:25, a dilution of the sample would be needed with additional method optimization. This is a good example demonstrating the necessity for independent linearity evaluation of each molecule to adapt to different mAb mixtures in FDC products with wide ratios.

For the novel methodology reported in this paper, the two molecules in combination did not show any overlapping peaks due to their dissimilarities in pI, thus, facilitating data analysis of the charge variants belonging to each molecule. We are currently evaluating strategies to analyze FDC products containing molecules with pI's close in value. One approach, where overlapping charge variant peaks cannot be resolved, peak grouping can be utilized to track changes in charge variants for QC testing. The drawback to this approach is the inability to distinguish molecule specific changes in the mixture. With the emergence of new technologies, such as Blaze™ and CEInfinite© with direct iCIEF to mass spectrometry sample injection, peak identification and characterization may be possible [42–44]. A second approach is to optimize the master mix components, including the use of chemical "spacers", to further separate the two molecules for analysis. However, this may be challenging due to lack of appropriate reagents to provide the necessary resolving power.

Concluding remarks

Leveraging simultaneous monitoring of fluorescence and UV absorbance, the iCIEF methodology proposed herein enables concurrent quantification of charge variants for FDC products with differing pI's and wide ratios up to 1:40. Qualification of the novel method included repeatability, linearity, and accuracy (recovery) modules. Determining linearity for both detection modes is required for each component in the FDC products during method development. This methodology avoids sample precipitation or capillary clogging issues caused by sample overloading using conventional protocols with only UV detection. This approach requires only a single sample preparation; therefore, the analyst does not need to prepare and analyze two different sample dilutions and then combine the results. This provides an efficient, reliable, reproducible, and QC friendly method for combination product testing.

Acknowledgements

The authors would like to acknowledge Dr. Hongji Liu for rigorous review of the manuscript.

Conflict of Interest

The authors have declared no conflict of interest.

Data Availability Statement

The data that support the findings of this study are available from the corresponding author upon reasonable request.

References

[1] Wang D, Nowak C, Mason B, Katiyar A, Liu H. Analytical artifacts in characterization of recombinant monoclonal antibody therapeutics. J Pharm Biomed Anal. 2020;183:113131–9.
[2] Lin J, Tan Q, Wang S, A high-resolution capillary isoelectric focusing method for the determination of therapeutic recombinant monoclonal antibody. J Sep Sci. 2011;34:1696–702.
[3] Liu H, Ponniah G, Zhang HM, Nowak C, Neill A, Gonzalez-Lopez N, Patel R, Cheng G, Kita AZ, Andrien B. *In vitro* and *in vivo* modifications of recombinant and human IgG antibodies. MAbs. 2014;6:1145–54.
[4] Sha S, Agarabi C, Brorson K, Lee DY, Yoon S. N-glycosylation design and control of therapeutic monoclonal antibodies. Trends Biotechnol. 2016;34:835–46.
[5] He XZ, Que AH, Mo JJ. Analysis of charge heterogeneities in mAbs using imaged CE Electrophoresis. 2009;30:714–22.
[6] Liu H, Ren W, Zong L, Zhang J, Wang Y. Characterization of recombinant monoclonal antibody charge variants using WCX chromatography, icIEF and LC-MS/MS. Anal Biochem. 2019;564–565:1–12.
[7] Anderson CL, Wang Y, Rustandi RR. Applications of imaged capillary isoelectric focussing technique in development of biopharmaceutical glycoprotein-based products. Electrophoresis. 2012;33:1538–44.
[8] Salas-Solano O, Kennel B, Park SS, Roby K, Sosic Z, Boumajny B, Free S, Reed-Bogan A, Michels D, McElroy W, Bonasia P, Hong M, He X, Ruesch M, Moffatt F, Kiessig S, Nunnally B. Robustness of iCIEF methodology for the analysis of monoclonal antibodies: an interlaboratory study. J. Sep. Sci. 2012;35:3124–9.
[9] Fekete S, Beck A, Fekete J, Guillarme D. Method development for the separation of monoclonal antibody charge variants in cation exchange chromatography, Part II: pH gradient approach. J Pharm Biomed Anal. 2015;102:282–9.
[10] Fekete S, Beck A, Fekete J, Guillarme D. Method development for the separation of monoclonal antibody charge variants in cation exchange chromatography, Part I: salt gradient approach. J Pharm Biomed Anal. 2015;102:33–44.
[11] Fekete S, Beck A, Veuthey JL, Guillarme D. Ion-exchange chromatography for the characterization of biopharmaceuticals. J Pharm Biomed Anal. 2015;113:43–55.

This article is protected by copyright. All rights reserved.

[12] Kahle J, Zagst H, Wiesner R, Wätzig H. Comparative charge-based separation study with various capillary electrophoresis (CE) modes and cation exchange chromatography (CEX) for the analysis of monoclonal antibodies. J Pharm Biomed Anal. 2019;174:460–70.
[13] Goyon A, Francois YN, Colas O, Beck A, Veuthey JL, Guillarme D. High-resolution separation of monoclonal antibodies mixtures and their charge variants by an alternative and generic CZE method. Electrophoresis. 2018;39:2083–90.
[14] Fekete S, Guillarme D, Sandra P, Sandra K. Chromatographic, Electrophoretic, and Mass Spectrometric Methods for the Analytical Characterization of Protein Biopharmaceuticals. Anal Chem. 2016;88:480–507.
[15] Sosic Z, Houde D, Blum A, Carlage T, Lyubarskaya Y. Application of imaging capillary IEF for characterization and quantitative analysis of recombinant protein charge heterogeneity. Electrophoresis. 2008;29:4368–76.
[16] Beck A, Wagner-Rousset E, Ayoub D, Van Dorsselaer A, Sanglier-Cianférani S. Characterization of therapeutic antibodies and related products. Anal Chem. 2013;85:715–36.
[17] Felten C, Salas-Solano O, Michels DA , Imaged Capillary Isoelectric Focusing for Charge-Variant Analysis of Biopharmaceuticals. BioProcess Int. 2011;9:48–54.
[18] Zhang X, Chemmalil L, Ding J, Mussa N, Li Z. Imaged capillary isoelectric focusing in native condition: A novel and successful example. Anal Biochem. 2017;537:13–9.
[19] Zhang X, Voronov S, Mussa N, Li Z. A novel reagent significantly improved assay robustness in imaged capillary isoelectric focusing. Anal Biochem. 2017;521:1–7.
[20] Rustandi RR, Anderson C, Hamm M. Application of Capillary Electrophoresis in Glycoprotein Analysis in: Beck A (Ed.) Chapter 11 Glycosylation Engineering of Biopharmaceuticals: Methods in Molecular Biology, vol.968, New York: Springer Science+Business Media; 2013. pp. 181–197.
[21] Dadouch M, Ladner Y, Perrin C. Analysis of Monoclonal Antibodies by Capillary Electrophoresis: Sample Preparation, Separation, and Detection. Separations. 2021;8:4–33.
[22] Radenović DČ, de Kort BJ, Somsen GW. Lamp-based native fluorosecne detection of proteins in capillary electrophoresis. J Chromatogr A. 2009;1216:4629–32.
[23] Chan KC, Veenstra TD, Issaq HJ. Comparison of Fluorescence, Laser-Induced Fluorescence, and Ultraviolet Absorbance Detection for Measuring HPLC Fractionated Protein/Peptide Mixtures. Anal Chem. 2011;83:2394–6.
[24] Goyon A, Excoffier M, Janin-Bussat MC, Bobaly B, Fekete S, Guillarme D, Beck A. Determination of isoelectric points and relative charge variants of 23 therapeutic monoclonal antibodies. J Chromatogr B Anal Technol Biomed Life Sci. 2017;1065–1066:119–28.
[25] Ahluwalia D, Belakavadi M, Das TK, Katiyar A. A three-point identity criteria tool for establishing product identity using icIEF method. J Chromatogr B Anal Technol Biomed Life Sci. 2018;1083:271–7.
[26] Tang J, Shalabi A, Hubbard-Lucey VM. Comprehensive analysis of the clinical immuno-oncology landscape. Ann Oncol. 2018;29:84–91.
[27] Wolchok JD, Kluger H, Callahan MK, Postow MA, Rizvi NA, Lesokhin AM, Segal NH, Ariyan CE, Gordon RA, Reed K, Burke MM, Caldwell A, Kronenberg SA, Agunwamba BU, Zhang X, Lowy I,

This article is protected by copyright. All rights reserved.

Inzunza HD, Feely W, Horak CE, Hong Q, Korman AJ, Wigginton, JM, Gupta A, Sznol M. Nivolumab plus ipilimumab in advanced melanoma. N Engl J Med. 2013;369:122–33.

[28] Henricks LM, Schellens JH, Huitema AD, Beijnen JH. The use of combinations of monoclonal antibodies in clinical oncology. Cancer Treat Rev. 2015;41:859–67.

[29] Selby MJ, Engelhardt JJ, Johnston RJ, Lu LS, Han M, Thudium K, Yao D, Quigley M, Valle J, Wang C, Chen B, Cardarelli PM, Blanset D, Korman AJ. Preclinical Development of Ipilimumab and Nivolumab Combination Immunotherapy: Mouse Tumor Models, *In Vitro* Functional Studies, and Cynomolgus Macaque Toxicology. PLoS One. 2016;11: e0161779.

[30] Sadineni V, Quan Y, Kaserer W. Compositions Comprising a Combination of an Anti-PD–1 Antibody and Another Antibody. 2017;Pub. No. US 2016/0304607 A1.

[31] Mace TA, Shakya R, Pitarresi JR, Swanson B, McQuinn CW, Loftus S, Nordquist E, Cruz-Monserrate Z, Yu L, Young G, Zhong X, Zimmers TA, Ostrowski MC, Ludwig T, Bloomston M, Bekaii-Saab T, Lesinski GB, IL–6 and PD-L1 antibody blockade combination therapy reduces tumour progression in murine models of pancreatic cancer. Gut. 2018;67:320–32.

[32] Lipson EJ, Tawbi HAH, Schadendorf D, Ascierto PA, Matamala L, Gutiérrez EC, Rutkowski P, Gogas H, Lao CD, Menezes JJd, Dalle S, Arance AM, Grob JJ, Srivastava S, Abaskharoun M, Simonsen KL, Li B, Long GV, Hodi FS. Relatlimab (RELA) plus nivolumab (NIVO) versus NIVO in first-line advanced melanoma: Primary phase III results from RELATIVITY-047 (CA224-047). J Clin Oncol. 2021;39:9503.

[33] Kirschbrown WP, Wynne C, Kågedal M, Wada R, Li H, Wang B, Nijem I, Badovinac Crnjevic T, Gasser H, Heeson S, Eng-Wong J, Garg A. Development of a Subcutaneous Fixed-Dose Combination of Pertuzumab and Trastuzumab: Results From the Phase Ib Dose-Finding Study. J Clin Pharmacol. 2019;59:702–16.

[34] Sharma VK, Misra B, McManus KT, Avula S, Nellaiappan K, Caskey M, Horowitz J, Nussenzweig MC, Seaman MS, Javeri I, Dey AK. Characterization of Co-Formulated High-Concentration Broadly Neutralizing Anti-HIV–1 Monoclonal Antibodies for Subcutaneous Administration. Antibodies. 2020;9:36–51.

[35] Kim J, Kim YJ, Cao M, De Mel N, Albarghouthi M, Miller K, Bee JS, Wang J, Wang X. Analytical characterization of coformulated antibodies as combination therapy. MAbs. 2020;12:1738691.

[36] Loughney JW, Ha S, Rustandi RR. Quantitation of CRM197 using imaged capillary isoelectric focusing with fluorescence detection and capillary Western. Anal Biochem. 2017;534:19–23.

[37] Li X, Yu L, Shi X, Rao C, Zhou Y. Capillary isoelectric focusing with UV fluorescence imaging detection enables direct charge heterogeneity characterization of erythropoietin drug products. J Chromatogr A. 2021;1643:462043.

[38] Cao M, De Mel N, Shannon A, Prophet M, Wang C, Xu W, Niu B, Kim J, Albarghouthi M, Liu D, Meinke E, Lin S, Wang X, Wang J. Charge variants characterization and release assay development for co-formulated antibodies as a combination therapy. MAbs. 2019;11:489–99.

[39] International Conference on Harmonization of Technical Requirements for Registration of Pharmaceuticals for Human Use: Validation of Analytical Procedures: Text and Methodology Q2(R1). 2005.

[40] Improving Charge Variant Analysis with Maurice Native Fluorescence. ProteinSimple. 2017.

This article is protected by copyright. All rights reserved.

[41] Saidel LJ, Goldfarb AR, Waldman S. The absorption spectra of amino acids in the region two hundred to two hundred and thirty millimicrons. J Biol Chem. 1952;197:285–91.
[42] Mack S, Arnold D, Bogdan G, Bousse L, Danan L, Dolnik V, Ducusin M, Gwerder E, Herring C, Jensen M, Ji J, Lacy S, Richter C, Walton I, Gentalen E. A novel microchip-based imaged CIEF-MS system for comprehensive characterization and identification of biopharmaceutical charge variants. Electrophoresis. 2019;40:3084–91.
[43] Montealegre C, Neususs C. Coupling imaged capillary isoelectric focusing with mass spectrometry using a nanoliter valve. Electrophoresis. 2018;39:1151–54.
[44] Dai J, Lamp J, Xia Q, Zhang Y. Capillary Isoelectric Focusing-Mass Spectrometry Method for the Separation and Online Characterization of Intact Monoclonal Antibody Charge Variants. Anal Chem. 2018;90:2246–54.

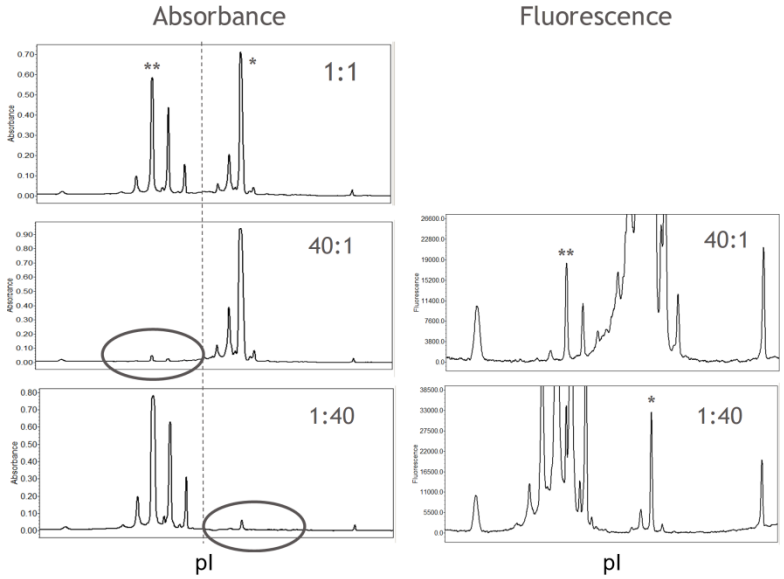

Figure 1. Analysis of mAb1:mAb2 mixtures with iCIEF using dual detection of absorbance at 280 nm and fluorescence. The areas in the circle are the expected regions of the charge variant peaks of the lower abundant species in the 40:1 and 1:40 mixtures, which are not quantifiable using absorbance. These species can be quantified using fluorescence. Asterisk (*) and double asterisk (**) represent the locations of the main peak of mAb1 and mAb2, respectively.

This article is protected by copyright. All rights reserved.

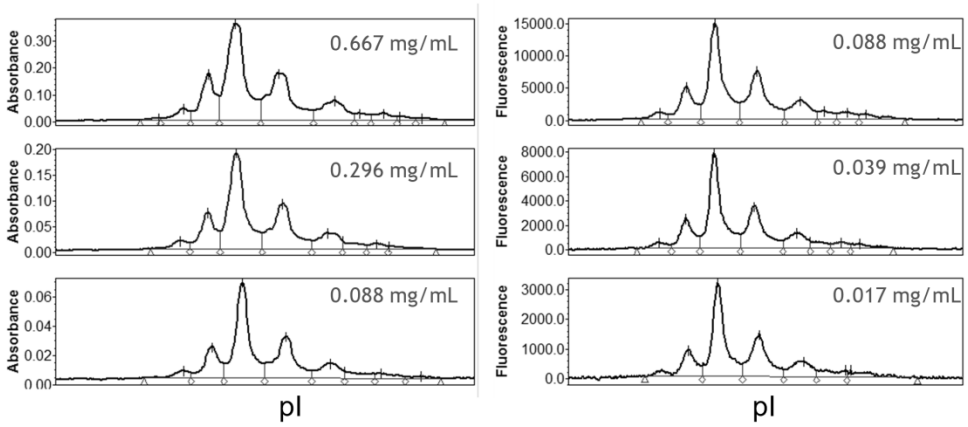

Figure 2. Electropherograms of iCIEF analysis of mAb3 covering sample concentrations of 0.017–0.667 mg/mL. The upper portion of the range (left, 0.088–0.667 mg/mL) was acquired with absorbance detection at 280 nm. The lower portion of the range (right, 0.017–0.088 mg/mL) was acquired with native fluorescence detection.

This article is protected by copyright. All rights reserved.

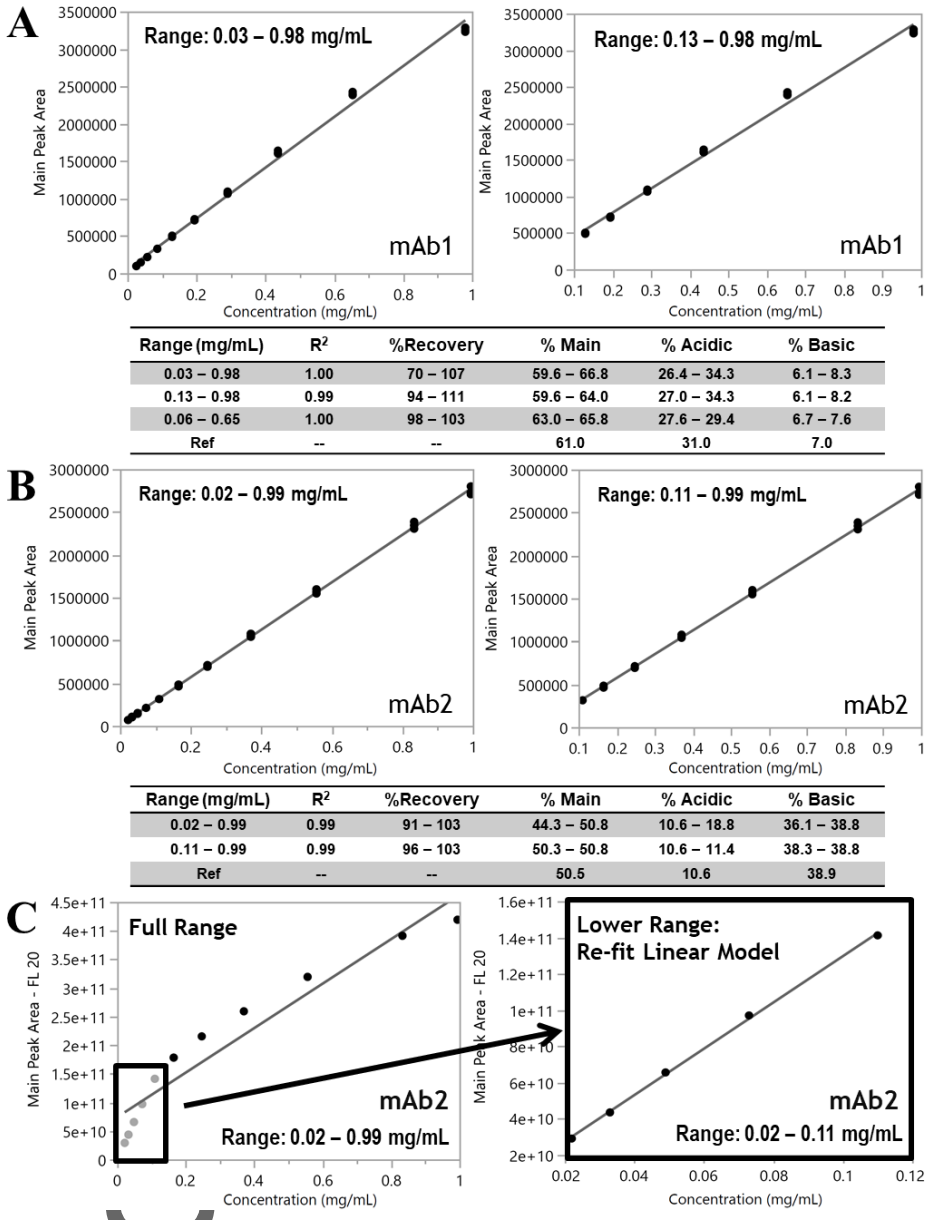

Range (mg/mL)	R^2	%Recovery	% Main	% Acidic	% Basic
0.03 – 0.98	1.00	70 – 107	59.6 – 66.8	26.4 – 34.3	6.1 – 8.3
0.13 – 0.98	0.99	94 – 111	59.6 – 64.0	27.0 – 34.3	6.1 – 8.2
0.06 – 0.65	1.00	98 – 103	63.0 – 65.8	27.6 – 29.4	6.7 – 7.6
Ref	--	--	61.0	31.0	7.0

Range (mg/mL)	R^2	%Recovery	% Main	% Acidic	% Basic
0.02 – 0.99	0.99	91 – 103	44.3 – 50.8	10.6 – 18.8	36.1 – 38.8
0.11 – 0.99	0.99	96 – 103	50.3 – 50.8	10.6 – 11.4	38.3 – 38.8
Ref	--	--	50.5	10.6	38.9

Figure 3. Absorbance linearity of main peak area for A) mAb1 and B) mAb2. Both mAbs show good linearity R^2 values across the entire final concentration range. However, by narrowing the range, recovery is improved for both mAbs. The values of the main, acidic, and basic relative area percentages are closer to the reference material (Ref) with the improved recovery compared to the wide range linear fits. Ranges of percent peak area for acidic, main, and basic are given for data obtained across the concentration range. C) Fluorescence linearity with 20 seconds exposure for main peak area of mAb2. From 0.02–0.99 mg/mL (final concentration), the signal gets saturated at

This article is protected by copyright. All rights reserved.

high concentrations. The data is linear at the lower concentration range from 0.02–0.11 mg/mL, as shown in the re-fit model.

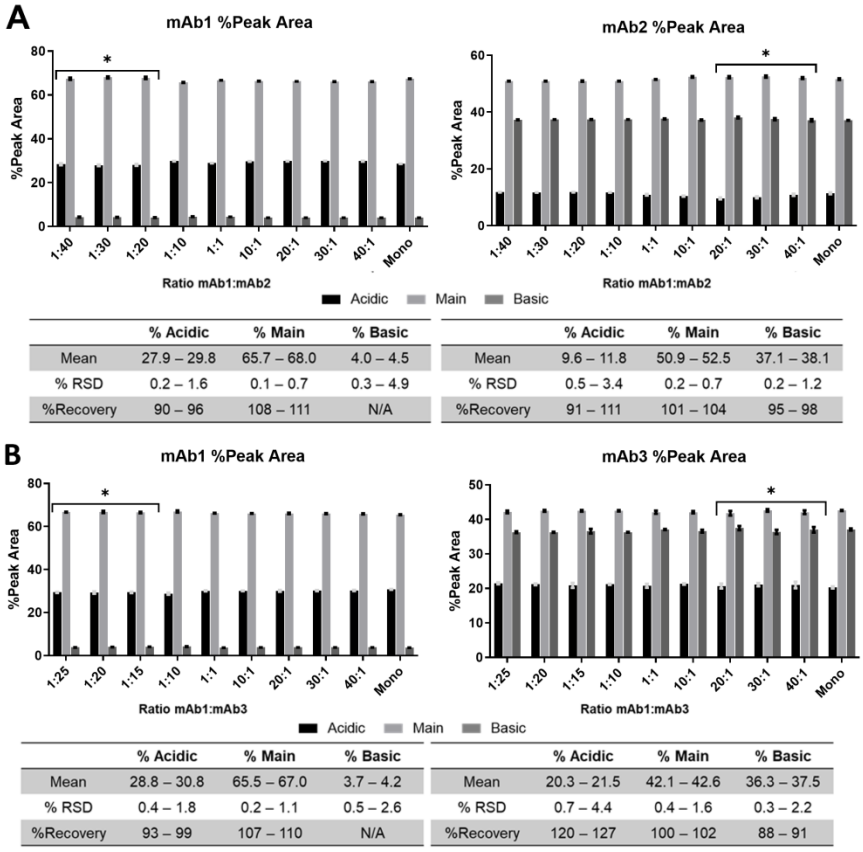

	% Acidic	% Main	% Basic
Mean	27.9 – 29.8	65.7 – 68.0	4.0 – 4.5
% RSD	0.2 – 1.6	0.1 – 0.7	0.3 – 4.9
%Recovery	90 – 96	108 – 111	N/A

	% Acidic	% Main	% Basic
Mean	9.6 – 11.8	50.9 – 52.5	37.1 – 38.1
% RSD	0.5 – 3.4	0.2 – 0.7	0.2 – 1.2
%Recovery	91 – 111	101 – 104	95 – 98

	% Acidic	% Main	% Basic
Mean	28.8 – 30.8	65.5 – 67.0	3.7 – 4.2
% RSD	0.4 – 1.8	0.2 – 1.1	0.5 – 2.6
%Recovery	93 – 99	107 – 110	N/A

	% Acidic	% Main	% Basic
Mean	20.3 – 21.5	42.1 – 42.6	36.3 – 37.5
% RSD	0.7 – 4.4	0.4 – 1.6	0.3 – 2.2
%Recovery	120 – 127	100 – 102	88 – 91

Figure 4. Proof-of-concept iCIEF method for FDC products of A) mAb1:mAb2 from 1:40 to 40:1 and B) mAb1:mAb3 from 1:25 to 40:1. In A, data is shown for mAb1 (left) and mAb2 (right) percent peak area. In B, data is shown for mAb1 (left) and mAb3 (right) percent peak area. %RSD values (presented as error bars) are calculated from three independent preparations of each ratio. Minimum and maximum ranges are given for mean and %RSD values from results obtained across all ratios. Due to the low area percent of the basic group of mAb1, the percent recovery is reported as "N/A". Asterisk (*) designates data obtained with fluorescence with 20 seconds exposure; all other data obtained with absorbance at 280 nm.

This article is protected by copyright. All rights reserved.